Songklanakarin J. Sci. Technol.
46 (1), 61–67, Jan. – Feb. 2024

http://www.sjst.psu.ac.th

Original Article

Evaluation of contact stress distribution on the surface of tibial insert component: Finite element analysis

Techin Seechaipat[1], Supakit Rooppakhun[2*], and Chotchuang Phombut[2]

[1] *School of Biomedical Innovation Engineering, Institute of Engineering, Suranaree University of Technology, Mueang, Nakhon Ratchasima 30000, Thailand*

[2] *School of Mechanical Engineering, Institute of Engineering, Suranaree University of Technology, Mueang, Nakhon Ratchasima 30000, Thailand*

Received: 27 January 2022; Revised: 13 February 2024; Accepted: 16 February 2024

Abstract

The purpose of this study was to evaluate and compare the contact stress distributions on the surface of the tibial insert between the posterior-stabilized (PS) and cruciate-retaining (CR) total knee arthroplasty (TKA). 3D finite element (FE) model of a femoral and the tibial insert component was constructed and analyzed using computer software. The results showed that the contact stress distribution on the tibial insert depends on the flexion angle. The maximum magnitude of contact stress in the PS TKA was higher than in the CR TKA, while the contact area of the former was lower than that of the latter. In addition, the results of FE simulations were similar to results from mechanical test using the Fujifilm technique. This study can explain differences between the two types of TKA, observing the behavior of the contact mechanism based on the contact knee test.

Keywords: contact stress, tibial insert, total knee arthroplasty, finite element analysis

1. Introduction

Total knee arthroplasty (TKA) to treat osteoarthritis is a standard orthopedic surgical treatment that restores the weight-bearing surfaces of the knee joint. However, there are still reports of complications from patients after surgery due to implant loosening, pain, and weight-bearing surface wear (Ardestani *et al.*, 2015; Koh, Lee, & Kang, 2019a). Previous studies have suggested that the wear of ultra-high molecular weight polyethylene (UHMWPE) of tibial inserts is an essential factor shortening the lifetime of TKA and loosening it (Koh, Lee, & Kang, 2019a; Naudie, Ammeen, Engh, & Rorabeck, 2007). However, the rate of revision resulting from wear is now significantly lower because UHMWPE wear resistance was improved, and the amount of wear was reduced (Sharkey, Lichstein, Shen, Tokarski, & Parvizi, 2014). The mechanical wear is related to the contact stress distribution proportional to the bearing load, and it varies with knee flexion angle, wear coefficient factor, and kinematics of sliding distance (Abdelgaied *et al.*, 2014; Netter *et al.*, 2016). Mechanical factors that cause wear in TKR include material, geometric shape of insert design, and kinematics of daily activity. Several experimental approaches have been used to evaluate the wear of polyethylene inserts using the conventional wear tester (Camacho, González, Espinosa, Mondragón, & Stafford, 2021; Naudie, Ammeen, Engh, & Rorabeck, 2007; Netter *et al.*, 2015). Before the dynamic wear test, evaluating the level and distribution of contact pressure was done in a preliminary prediction of the level and location of tibial insert wear (Galvin *et al.*, 2009; Murakami *et al.*, 2018).

Generally, TKA is classified into two categories based on functional design: posterior stabilized (PS) or cruciate-retaining (CR) (Ardestani *et al.*, 2015; Broberg, Ndoja, MacDonald, Lanting, & Teeter, 2020). In the CR-type, the posterior cruciate ligament (PCL) is retained to maintain knee kinematics as natural as possible. On the other hand, the PS-type eliminates the PCL instead of resected PCL; the cam-post mechanism of the tibial insert was introduced in the PS-type. The mechanism provides a constraint that limits anterior

*Corresponding author
Email address: supakit@sut.ac.th

translation of the femur on the tibia during flexion and ensures femoral rollback with progressive knee flexion (Koh, Son, Kwon, Kwon, & Kang, 2019b). However, clinical studies have reported no difference between CR- and PS-type TKA and have clarified the difference between the two types of implants (Migliorini, Eschweiler, Tingart, & Rath, 2019; Tanzer, Smith, & Burnett, 2002). CR-type TKA advocates commented that retaining the PCL provides more natural knee kinematics and improved proprioception-enhanced inherent stability, including reducing the shear forces on the tibia (Rajgopal *et al.*, 2017; Takagi *et al.*, 2017). The disadvantages include difficulty in obtaining a balanced PCL in the face of a deficient PCL, which is also reported as a significant cause of CR-type's instability (Mazzucchelli *et al.*, 2016). In the PS-type design the PCL was sacrificed and replaced with post-cam mechanics, and advocates claim that this allows for better ligament balancing and straightforward surgical procedures, including reduced tibiofemoral loads and more predictable kinematics (Broberg, Ndoja, MacDonald, Lanting, & Teeter, 2020; Mazzucchelli *et al.*, 2016). In addition, using PS-type is associated with resectioning a significant amount of bone and soft tissues from the femur bone (Mazzucchelli *et al.*, 2016; Rajgopal *et al.*, 2017).

The contact pressure distribution of TKA was determined based on the standard specification for knee replacement prosthesis according to ASTM F2083. On the tibiofemoral joint of the TKA, contact stress distribution and contact area were evaluated using 4 to 5 times the bodyweight load in different flexion angles, with 0, 15, 30, 60, and 90 degrees recommended. The contact stress distribution is generally evaluated by various methods, such as using Fuji pressure-sensitive film, the K-scan system, and finite element (FE) analysis (Halloran, Petrella, & Rullkoetter, 2005; Murakami *et al.*, 2018). Fuji film techniques have been widely used to measure contact mechanics in the TKA; however, there are also disadvantages in measuring contact mechanics in real-time and reproducible techniques (Dharia, Snyder, & Bischoff, 2020; Zdero, Fenton, Rudan, & Bryant, 2001). A computational model based on FE analysis has been introduced, as an alternative approach to investigate the contact mechanics of the TKA, to address the limitations of mechanical testing. FE analysis provides an efficient toolset to evaluate TKA design under various loading conditions (Ardestani *et al.*, 2015; Halloran, Petrella, & Rullkoetter, 2005; Shu, Yao, Yamamoto, Sato, & Sugita, 2021). Therefore, this study aimed to evaluate and compare the contact stress distributions on the surface of the tibial insert between the PS and CR-types of total knee arthroplasty. Validation of the FE analysis was also performed using the Fuji film technique. We hypothesize that PS- and CR-type TKAs differ in contact stress and contact area. This information can be used to design and develop knee prostheses for reduced contact stress.

2. Materials and Methods

2.1 Three-dimensional (3D) model of TKA

Commercial TKA models, including PS- and CR-type (Implantcast, ACS size 4), were scanned with a 3D scanner (Handy Scan 3D, Creaform, Levis, Canada). The data were then applied to construct a three-dimensional (3D) model using Geomagic Design X software (3D System, LUXEMBOURG) and SolidWorks software (Dassault Systems), as shown in Figure 1.

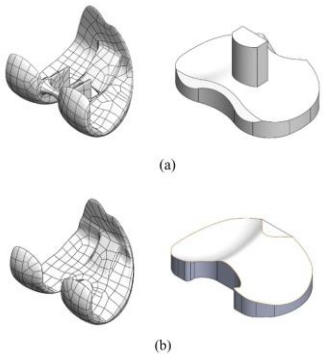

Figure 1. The 3D model of TKA consisted of the femoral component and tibial insert: (a) PS-type, and (b) CR-type.

2.2 Finite-element (FE) modeling and boundary conditions

Figure 2(a) illustrates a 3D FE model of the femoral and tibial insert components considered rigid and deformable, respectively. Linearly elastic isotropic material with a modulus of 685 MPa and a Poisson ratio of 0.46 was used for the UHMWPE tibial component (Bei, Fregly, Sawyer, Banks, & Kim, 2004; Dharia, Snyder, & Bischoff, 2020). The analysis was based on computerized simulation software, ABAQUS KNEE Simulator (AKS; Dassault Systèmes SE, France).

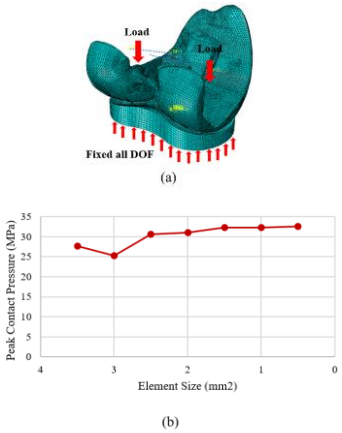

Figure 2. The finite element analysis. (a) 3D FE model of TKA and boundary conditions, and (b) convergence test by mesh refinement

For the boundary conditions, the bearing compressive load was created as the body weight with equal distribution on the medial and lateral sides of the femoral component under various flexion angles, as shown in Table 1. The femoral component was allowed freedom of moving in medial-lateral translation, including internal-external and varus-valgus rotations. The bottom surface of the tibial insert was considered a fixed support by restricting all translation and rotation degrees of freedom. The coefficient of friction between the femoral component and the tibial insert was 0.04 (Naudie, Ammeen, Engh, & Rorabeck, 2007).

Table 1. The load at each flexion angle according to standard specifications

Flexion angle (degrees)	Load (N)
0	2901
15	2901
30	3267
60	3626
90	3267

Convergence testing was performed to verify that the solution did not exhibit any significant changes with mesh refinement, as shown in Figure 2(b). The convergence study results indicated that the mesh density utilized for these insert components was acceptable relative to that obtained in a previous study (Koh, Lee, & Kang, 2019a; Koh, Son, Kwon, Kwon, & Kang, 2019b). The element edge length was controlled (in the range from 3.5 mm to 0.5 mm) until the percentage difference in the critical results of maximum contact stress between two consecutive mesh densities was less than 2% of the peak contact pressure.

2.3 Experimental method

Figure 3 displays the mechanical apparatus consisting of upper and lower fixtures. The lower fixture was specifically designed to allow movement in rotation. A rotation axis was defined by the connection between the centers of the medial and lateral circles generated by the circular fitting of the femoral condyles. It is possible to adjust the flexion angle of the lower fixture by removing the pin from the femoral holder, rotating the femoral holder to the desired angle, and inserting the pin in a small hole, as shown in Figure 3(b). The applied load was controlled with equal distribution evenly in the medial and lateral parts of the tibial insert. The upper fixture was used to attach to a Universal Testing Machine (UTM) (Instron, Model 5565). The load in each flexion angle, according to standard specifications for testing a knee replacement prosthesis, is shown in Table 1. The mono-sheet Fuji film type (Medium pressure, Fuji Photo Film, Tokyo, Japan) was inserted between the femoral and tibial parts to measure the contact stress and area. The contact pad between the femoral and tibial components was held for two minutes during the applied load.

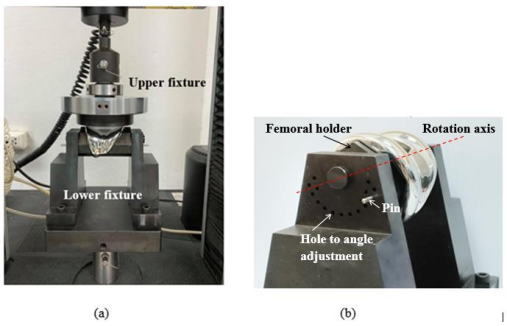

Figure 3. The mechanical apparatus. (a) The experimental configuration for the contact test using the Fuji film technique, and (b) mechanism for adjusting the angle of the lower fixture

The Fuji film contact sheet was scanned with a resolution of 1,000 dpi using the color image scanner Epson A4 Perfection V37 (Epson, Perfection V37). The result of pressure distribution was displayed using mapping system software (FPD-8010E, Fuji Photo Film, Japan). The contact film was used within 10 MPa to 50 MPa, and the temperature ranged from 20° to 35°C.

3. Results and Discussion

3.1 The results of the FE analysis

Figure 4 shows the FE analysis results of the PS- and CR-type contact stress distributions by flexion angle. Figures 5(a) and 5(b) display comparative results of the maximum contact stress and the contact area between PS- and CR-types by flexion angle. The maximum contact stress of the PS-TKA was in the range from 33.5 MPa to 77.82 MPa, while for CR-TKA it ranged from 26.22 MPa to 38.7 MPa, for flexion angles from 0 to 90 degrees. Regarding the contact area, the results show that both models had contact decrease with flexion angle. Comparatively, the maximum contact stress displayed in the PS-type was higher than in the CR-type, at any given flexion angle. However, the contact area of the PS-type was smaller than that of the CR-type at all flexion angles. The contact area of the CR-type has an elliptical shape and is more expanded than in the PS-type. For the PS-type, the contact area is displayed on a region of post-cam mechanics during a knee flexion angle of approximately 48 degrees. As the flexion angle increases, both types of TKA have a diminishing contact area.

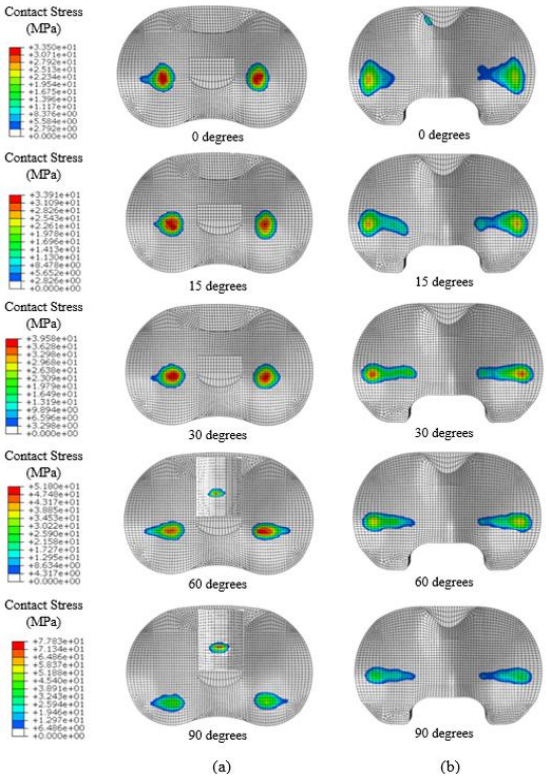

Figure 4. Typical contact stress distributions on the tibial insert at each flexion angle. (a) PS-type, and (b) CR-type

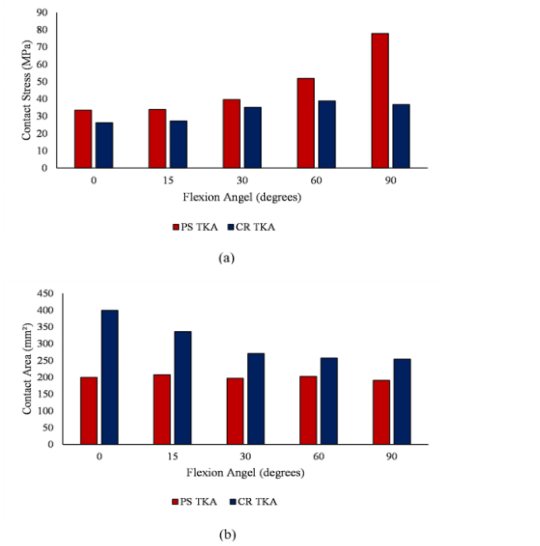

Figure 5. Comparative results of (a) maximum contact stress, and (b) contact area between PS- and CR-types of TKA at each flexion angle

Additionally, the position of the contact area in PS-type shifted to posterior direction more than in CR-type when there were high flexion angles. Therefore, the PS-type tended to loosen at high flexion angles, whereas the CR-type hardly changed. According to the results, the magnitude of contact stress increases. In contrast, the contact area decreases when there are high flexion angles.

Figure 6 shows the maximum von Mises stress in PS- and CR-types of TKA for each flexion angle. The magnitude of von Mises stress in the PS TKA was higher than in CR TKA at flexion angles from 30 to 90 degrees. For both types the highest von Mises stress was exhibited at 90 degrees flexion angle. However, it did not exceed the yield strength of the material (in the range from 37 MPa to 43 MPa) (Camacho, González, Espinosa, Mondragón, & Stafford, 2021; Jin *et al.*, 2016; Koh, Lee, & Kang, 2019a; Takeuchi, Lathi, Khan, & Hayes, 1995).

According to the results, the CR-type was preferable for reducing the contact stress on the tibiofemoral joint while providing high conformity, including mobility (Cheng, Huang, Liau, & Huang, 2003). The CR-type in which posterior cruciate ligament was preserved had larger contact area than PS-type, and the post-cam mechanism was accommodated to improve functionality (Ardestani *et al.*, 2015; Broberg, Ndoja, MacDonald, Lanting, & Teeter, 2020). Therefore, the curved contact area between the tibiofemoral joints in PS was less than in the CR-type (Hofer, Gejo, McGarry, & Lee, 2012). Previous biomechanical studies have shown differences in load conditions resulting in various contact stresses. The determination of contact stress and contact area within seven different TKA based on a load of 2000 N has been determined using the Fuji film technique (Murakami *et al.*, 2018). The magnitude of maximum contact stress was found to be in the range from 0 MPa to 15 MPa for the flexion angle of 15 degrees; and from 20 MPa to 30 MPa for the flexion angle of 60 degrees. In addition, the effect of kneeling on tibiofemoral contact for CR- and PS-types was evaluated based on three different loading conditions at high

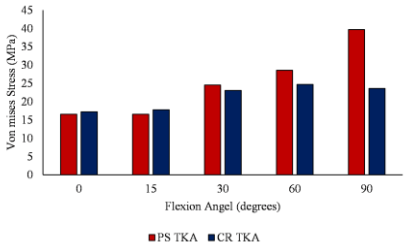

Figure 6. The maximum von Mises stress in PS- and CR-types of TKA

flexion angles (Hofer, Gejo, McGarry, & Lee, 2012). The maximum von Mises stresses in both types of TKA are within the acceptable range avoiding mechanical failure, based on the compressive yield strength, for knee joint loading in general daily activities. Generally, the tensile strength of UHMWPE materials is between 37 MPa and 43 MPa. The compressive strength is between 14 MPa and 83 MPa (Camacho, González, Espinosa, Mondragón, & Stafford, 2021; Jin *et al.*, 2016; Koh, Lee, & Kang, 2019a; Takeuchi, Lathi, Khan, & Hayes, 1995).

The study clearly showed the difference in contact stress and in contact area between the PS- and CR-types of TKA, based on the standard loading in various flexion angles. To specify the PS-type design, the post-cam mechanism was one of the contact surfaces that resulted in contact stress. The results show that the femoral cam contacted the anterior face of the post of the tibial insert in early flexion at approximately 48 degrees, affecting a posterior force applied on the post-cam. Generally, the contact of the post-cam mechanism was initially made at flexion angle of approximately 43 to 50 degrees (Pianigiani, Scheys, Labey, Pascale, & Innocenti, 2015). Previous studies have shown that contact stress at the post-cam mechanics increases when the knee flexion angle increases, during for example kneeling (Hofer, Gejo, McGarry, & Lee, 2012; Huang, Liau, Huang, & Cheng, 2006). The post-cam mechanism allows the PS-type of TKA to allow the backward rolling of the femoral component on the tibia insert more than the CR-type of TKA, in the range of flexion angles from 0 degrees to 135 degrees (Bellemans, Banks, Victor, Vandenneucker, & Moemans, 2002). Many studies have shown the post-cam mechanism of PS-type as an essential consideration in TKA design (Koh, Son, Kwon, Kwon, & Kang, 2019b).

The contact stress distribution of PS-type displayed a circular shape, while the CR-type exhibited an ellipse shape. The difference in contact pressure shapes was due to the conformity, which is the ratio of curvature radii of the femur component and the tibial insert. The conformity of the PS-type matched both coronal and sagittal planes, resulting in a circular contour. In CR the conformity in the sagittal plane was matched, but the conformity in the coronal plane was flattened, giving the contour shape an ellipse. In the TKA design, most studies indicated that the low conformity between the femoral component and a tibial insert should be recommended for substantially reduced wear on the knee implant (Abdelgaied *et al.*, 2014; Galvin *et al.*, 2009). A previous study evaluated wear performance concerning different conformities of tibia insert surfaces in PS-type. The design should carefully consider the tibiofemoral surface conformity, especially when one plane of curvature is matched. The case where the other is flattened exhibits the

lowest volumetric wear (Koh, Son, Kwon, Kwon, & Kang, 2019b). There is also a study on the post-cam positioning mechanism in the PS-type against wear. The anterior placement of the post in PS-type adversely affects polyethylene wear and damage (Indelli, Marcucci, Graceffa, Charlton, & Latella, 2014). However, cam-post placement and design changes also depend on their relation to the shape and location of the tibial surfaces.

3.2 Validation of FE results

Figures 7 and 8 exhibit comparative results on contact area and contact stress at each flexion angle, between the FE analysis and Fuji film experiments. Figures 7(a) and 7(b) display comparative results on contact area between FE analysis and Fujifilm test, showing differences between 1.9 % and 3.6%, and 6.9% and 14.5%, for the medial and lateral sides, respectively. The difference in maximum contact stress between the FE analysis and the Fuji film test was in the range from 17.1% to 29.2%, and from 6% to 25.7% for respectively the medial and lateral sides, as shown in Figures 8(a) and 8(b).

Figures 9(a) and 9(b) display results on contact stress distributions on the surface of the tibial insert component for each flexion angle, obtained from FE analysis and Fuji film test, respectively. It can be noted that the distribution of contact stress was roughly circular on both the medial and lateral sides. The comparative results of contact phenomena for both methods were similar; however, the contact area obtained in the Fujifilm test was slightly more elongated and elliptical than in the FE analysis, on both medial and lateral sides.

Previous studies have revealed that Fuji film technique for contact stress, including the contact area in the tibiofemoral joint, has an accuracy range from 6 % to 36% (Dharia, Snyder, & Bischoff, 2020; Liau, Cheng, Huang, & Lo, 2002; Murakami *et al.*, 2018). Although the validation using Fuji film technique was variable and had a wide range, the most significant advantage of Fuji film is that the method has been evaluated numerous times and for a wide range of uses (Sarwar *et al.*, 2017). Computer simulations are among the tools for predicting contact mechanics outcomes. However, the FE model has errors from many causes. For example, the material models in this study are based on linearly elastic materials, while the real behavior is non-linearly elastic.

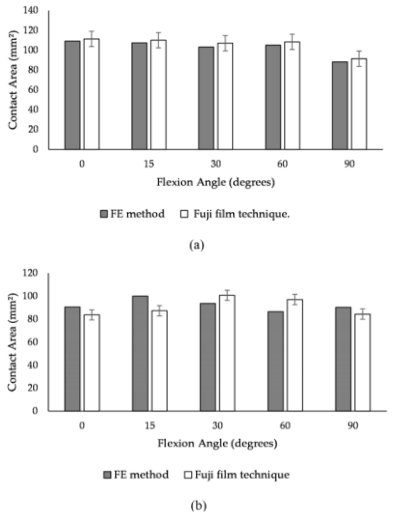

Figure 7. Comparative results on contact area between FE analysis and Fuji film technique at each flexion angle. (a) Medial side, and (b) lateral side

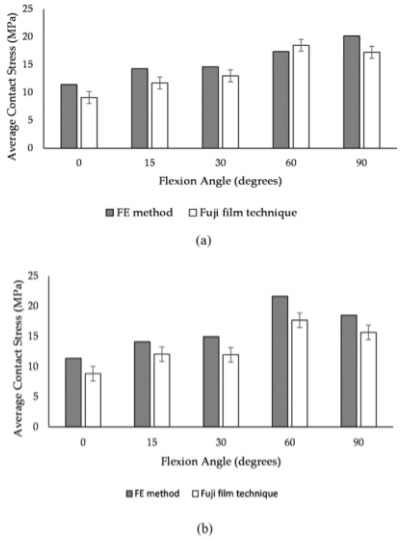

Figure 8. Comparative results on average contact stress between FE analysis and Fuji film technique at each flexion angle. (a) Medial side, and (b) lateral side

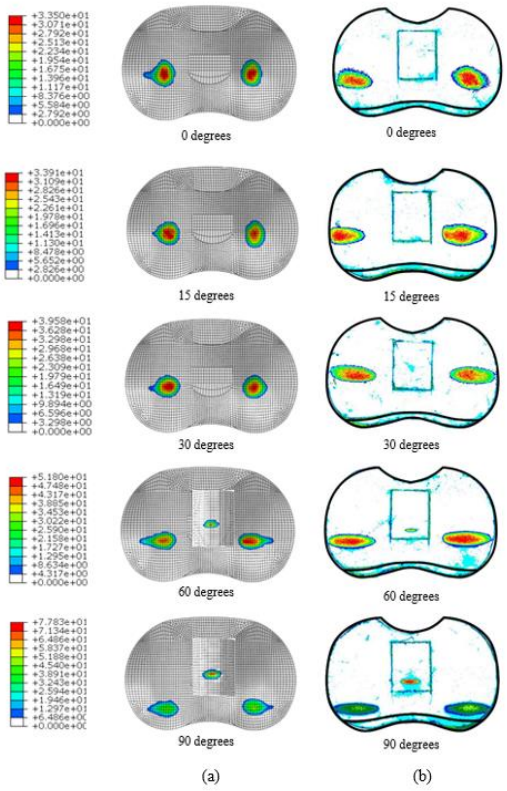

Figure 9. Results on contact stress distribution on the surface of tibial insert at each flexion angle (in MPa). (a) FE analysis, and (b) Fuji film technique

Furthermore, the material properties for the FE analysis were derived from previous studies rather than mechanical tests. Consequently, there are differences in the results between simulations and experiments. Furthermore, it was necessary to verify the boundary conditions and the modeling geometry, including the refinement of element size. Additionally, errors in experimental results could stem from the placing of Fuji film on the tibial insert surface, because the curvature of the tibial insert may be wrinkling the film. However, computer simulations offer several advantages, in examining different conditions and investigating outcomes. Moreover, the low cost and the rapid execution are advantages of modeling and simulation techniques, along with predicting specific results that experimentation cannot explain. However, this study has some limitations that need discussion. Firstly, this study's CR- and PS-type TKA models are all from one commercial manufacturer. Different designs of TKA components affect how contact stress is distributed. For instance, the curve of the femoral component has been designed in different ways, such as J-curves, single-radius curves, and multi-radius curves. Secondly, the distribution of contact pressure was evaluated in this study based on the assumption of static loading. The actual load in the knee joint during movement is dynamic, which includes multiple types of loads such as axial load, anterior-posterior load, and internal-external moment. A dynamic load can be applied according to standard loading profiles (ASTM F3141). In this study, the UTM tool had controlled load in one direction, unlike in the knee joint simulator in which there are controlled loads in multiple directions. Thirdly, the load sharing in this study used equal distribution of the force between medial and lateral because of easy control in the experiments, which is incorrect and does not match the biomechanical characteristics of the knee. Usually, 45-55% or 40-60% is used due to the knee's biomechanical characteristics (Park *et al.*, 2021). Finally, the load and displacement conditions of the knee joint should be considered in a system of muscles and ligaments that affect knee movement. Therefore, future studies should be conducted to provide insights into the contact mechanisms in knee implants similar to those of a typical knee joint.

4. Conclusions

The contact mechanisms on the surfaces of the tibial insert significantly differed between PS- and CR-types of TKA. The PS-type TKA displayed a higher peak magnitude of contact stress than the CR-type, and a lower contact area than in the CR-type. A knee implant's design can affect the contact stress and the contact area. According to validation results, the FE analysis of contact stress and contact area were similar to those in mechanical Fuji film tests. This information can be used to design and develop knee prostheses.

Acknowledgements

The authors thank Suranaree University of Technology, Suranaree University of Technology Hospital, and Engineering Institute. The author would like to thank the Center for Scientific and Technological Equipment staff at Suranaree University of Technology for supporting testing tools. This work could not have been done without the cooperation of the working team of orthopedic surgeons.

References

Abdelgaied, A., Brockett, C. L., Liu, F., Jennings, L. M., Jin, Z., & Fisher, J. (2014). The effect of insert conformity and material on total knee replacement wear. *Proceedings of the Institution of Mechanical Engineers, Part H: Journal of Engineering in Medicine, 228*(1), 98-106.

American Society for Testing and Materials (2021). Standard specification for knee replacement prosthesis, ASTM F2083-21. Retrieved from https://www.astm.org/f2083-21.html

American Society for Testing and Materials (2017). Standard guide for total knee replacement loading profiles, ASTM F3141-17a. Retrieved from https://www.astm.org/f3141-17a.html

Ardestani, M. M., Moazen, M., Maniei, E., & Jin, Z. (2015). Posterior stabilized versus cruciate-retaining total knee arthroplasty designs: Conformity affects the performance reliability of the design over the patient population. *Medical Engineering and Physics, 37*(4), 350-360.

Bei, Y., Fregly, B. J., Sawyer, W. G., Banks, S. A., & Kim, N. H. (2004). The relationship between contact pressure, insert thickness, and mild wear in total knee replacements. *Computer Modeling in Engineering and Sciences, 6*(2), 145-152.

Bellemans, J., Banks, S., Victor, J., Vandenneucker, H., & Moemans, A. (2002). Fluoroscopic analysis of the kinematics of deep flexion in total knee arthroplasty. Influence of posterior condylar offset. *The Bone and Joint Journal, 84*(1), 50-53.

Broberg, J. S., Ndoja, S., MacDonald, S. J., Lanting, B. A., & Teeter, M. G. (2020) Comparison of contact kinematics in posterior-stabilized and cruciate-retaining total knee arthroplasty at long-term follow-up. *The Journal of Arthroplasty, 35*(1), 272-277.

Camacho, N., González Carmona, J. M., Espinosa Arbeláez, D., Mondragón, G. C., & Stafford, S. (2021). UHMWPE in total knee arthroplasty: successes and failures. *Revista Colombiana de Materiales, 0*(16), 3-28.

Cheng, C. K., Huang, C. H., Liau, J. J., & Huang, C. H. (2003). The influence of surgical malalignment on the contact pressures of fixed and mobile bearing knee prostheses-a biomechanical study. *Clinical Biomechanics, 18*(3), 231-236.

Dharia, M. A., Snyder, S., & Bischoff, J. E. (2020). Computational model validation of contact mechanics in total ankle arthroplasty. *Journal of Orthopaedic Research, 38*, 1063-1069.

Galvin, A. L., Kang, L., Udofia, I., Jennings, L. M., McEwen, H. M. J., Jin, Z., & Fisher, J. (2009). Effect of conformity and contact stress on wear in fixed-bearing total knee prostheses. *Journal of Biomechanics, 42*(12), 1898-1902.

Halloran, J. P., Petrella, A. J., & Rullkoetter, P. J. (2005). Explicit finite element modeling of total knee replacement mechanics. *Journal of Biomechanics, 38*, 323-331.

Hofer, J. K., Gejo, R., McGarry, M. H., & Lee, T. Q. (2012). Effects of kneeling on tibiofemoral contact pressure and area in posterior cruciate-retaining and posterior cruciate-sacrificing total knee arthroplasty. *The Journal of Arthroplasty, 27*, 620-624.

Huang, C. H., Liau, J. J., Huang, C. H., & Cheng, C. K. (2006). Influence of post-cam design on stresses on posterior-stabilized tibial posts. *Clinical Orthopaedics and Related Research, 450*, 150-156.

Indelli, P. F., Marcucci, M., Graceffa, A., Charlton, S., & Latella, L. (2014). Primary posterior stabilized total knee arthroplasty: Analysis of different instrumentation. *Journal of Orthopaedic Surgery and Research, 9*, 54.

Jin, X., Wang, W., Xiao, C., Lin, T., Bian, L., & Hauser, P. (2016). Improvement of coating durability, interfacial adhesion, and compressive strength of UHMWPE fiber/epoxy composites through plasma pre-treatment and polypyrrole coating. *Composites Science and Technology, 128*, 169-175.

Koh, Y. G., Lee, J. A., & Kang, K. T. (2019a). Prediction of wear on tibial inserts made of UHMWPE, PEEK, and CFR-PEEK in total knee arthroplasty using finite-element analysis. *Lubricants, 7*(4).

Koh, Y. G., Son, J., Kwon, O. R., Kwon, S. K., & Kang, K. T. (2019b). Tibiofemoral conformity variation offers changed kinematics and wear performance of customized posterior-stabilized total knee arthroplasty. *Knee Surgery, Sports Traumatology, Arthroscopy, 27*(4), 1213-1223.

Liau, J. J., Cheng, C. K., Huang, C. H., & Lo, W. H. (2002). Effect of fuji pressure sensitive film on actual contact characteristics of artificial tibiofemoral joint. *Clinical Biomechanics, 17*(9-10), 698-70.

Mazzucchelli, L., Deledda, D., Rosso, F., Ratto, N., Bruzzone, M., Bonasia, D. E., & Rossi, R. (2016). Cruciate retaining and cruciate substituting ultra-congruent insert. *Annals of Translational Medicine, 4*(1), 2-2.

Migliorini, F., Eschweiler, J., Tingart, M., & Rath, B. (2019). Posterior-stabilized versus cruciate-retained implants for total knee arthroplasty: a meta-analysis of clinical trials. *European Journal of Orthopaedic Surgery and Traumatology, 29*(4), 937-946.

Murakami, K., Hamai, S., Moro-oka, T., Okazaki, K., Higaki, H., Shimoto, & T., Nakashima, Y. (2018). Variable tibiofemoral articular contact stress in fixed-bearing total knee arthroplasties. *Orthopaedics and Traumatology: Surgery and Research, 104*(2), 177-183.

Naudie, D. D., Ammeen, D. J., Engh, G. A., & Rorabeck, C. H. (2007). Wear and osteolysis around total knee arthroplasty. *Journal of the American Academy of Orthopaedic Surgeons, 15*(1), 53-64.

Netter, J., Hermida, J., Flores-Hernandez, C., Steklov, N., Kester, M., & Lima, D. D. (2015). Prediction of wear in crosslinked polyethylene unicompartmental knee arthroplasty. *Lubricants, 3*(2), 381-393.

Park, H. J., Bae, T. S., Kang, S.-B., Baek, H. H., Chang, M. J., & Chang, C. B. (2021). A three-dimensional finite element analysis on the effects of implant materials and designs on periprosthetic tibial bone resorption. *PLoS One, 16*(2), e0246866.

Pianigiani, Scheys, Labey, Pascale, Innocenti, S., Scheys, L., . . . Innocenti, B. (2015). Biomechanical analysis of the post-cam mechanism in a TKA: comparison between conventional and semi-constrained insert designs. *International Biomechanics, 2*(1), 22-28.

Rajgopal, A., Aggarwal, K., Khurana, A., Rao, A., Vasdev, A., & Pandit, H. (2017). Gait parameters and functional outcomes after total knee arthroplasty using persona knee system with cruciate retaining and ultracongruent knee inserts. *The Journal of Arthroplasty, 32*(1), 87-91.

Sarwar, A., Srivastava, S., Chu, C., Machin, A., Schemitsch, E. H., Bougherara, H., . . . Zdero, R. (2017). Biomechanical measurement rrror can be caused by fujifilm thickness: A theoretical, experimental, and computational analysis. *BioMed Research International, 2017*, 4310314.

Sharkey, P. F., Lichstein, P. M., Shen, C., Tokarski, A. T., & Parvizi, J. (2014). Why are total knee arthroplasties failing today-has anything changed after 10 years? *Journal of Arthroplasty, 29*(9), 1774-1778.

Shu, L., Yao, J., Yamamoto, K., Sato, T., & Sugita, N. (2021). In vivo kinematical validated knee model for preclinical testing of total knee replacement. *Computers in Biology and Medicine, 132*, 104311.

Takagi, H., Asai, S., Sato, A., Maekawa, M., Kawashima, H., & Kanzaki, K. (2017). Case series report of navigation-based in vivo knee kinematics in total knee arthroplasty with a gradually reducing femoral radius design. *Annals of Medicine and Surgery, 17*, 33-37.

Takeuchi, T., Lathi, V. K., Khan, A. M., & Hayes, W. C. (1995). Patellofemoral contact pressures exceed the compressive yield strength of UHMWPE in total knee arthroplasties. *The Journal of Arthroplasty, 10*(3), 363-368.

Tanzer, M., Smith, K., & Burnett, S. (2002). Posterior-stabilized versus cruciate-retaining total knee arthroplasty: balancing the gap. *The Journal of arthroplasty, 17(7), 813-819.*

Zdero, R., Fenton, P. V., Rudan, J., & Bryant, J. T. (2001). Fuji film and ultrasound measurement of total knee arthroplasty contact areas. *The Journal of arthroplasty, 16*(3), 367-375.